

PACS numbers: 68.55.J-, 75.50.Tt, 75.60.-d, 75.70.-i, 81.20.Ev, 81.20.Fw, 81.40.Rs

## Time Dependence on Magnetic Properties of Nanomaterial Manganese–Zinc Ferrite ( $\text{Mn}_{0.8}\text{Zn}_{0.2}\text{Fe}_2\text{O}_4$ ) by Co-Precipitation Method

Djoko Kustono<sup>1</sup>, Poppy Puspitasari<sup>2,3</sup>, Wahono<sup>2,3</sup>,  
Aris Sandy Setya Ananda<sup>2</sup>, Maizatul Shima Shaharun<sup>3</sup>,  
and Alief Muhammad<sup>2</sup>

<sup>1</sup>*Mechanical Engineering Department, Engineering Faculty,  
State University of Malang,  
5, Semarang Str.,  
65145 Malang, East Java, Indonesia*

<sup>2</sup>*Center of Nano Research and Advanced Materials,  
State University of Malang,  
5, Semarang Str.,  
65145 Malang, East Java Indonesia*

<sup>3</sup>*Fundamental and Applied Science Department,  
University Technology Petronas,  
32610 Bandar Seri Iskandar, Perak, Malaysia*

Researches on manganese–zinc ferrite  $\text{Mn}_{0.8}\text{Zn}_{0.2}\text{Fe}_2\text{O}_4$  got popular due to its good magnetic properties as a soft magnetic material. Studies on  $\text{Mn}_{0.8}\text{Zn}_{0.2}\text{Fe}_2\text{O}_4$  magnetic properties, especially before and after the sintering process, are required to see its magnetic material characterisation. Therefore, this research focused on manganese–zinc ferrite  $\text{Mn}_{0.8}\text{Zn}_{0.2}\text{Fe}_2\text{O}_4$  characterisations using co-precipitation method with sintering time variations of 3, 4, and 5 hours at 1100°C. Base materials used in this research were manganese oxide (MnO), zinc oxide (ZnO), and iron oxide ( $\text{Fe}_2\text{O}_3$ ). XRD, SEM–EDX, and VSM tests were used to characterise phase, morphology, and magnetic properties.  $\text{Mn}_{0.8}\text{Zn}_{0.2}\text{Fe}_2\text{O}_4$  with 3, 4, and 5 hours holding time sintering process resulted in crystallite size changed into 70.4194 nm, 52.91546 nm, and 26.45 nm. During the holding time of sintering process, the single  $\text{Mn}_{0.8}\text{Zn}_{0.2}\text{Fe}_2\text{O}_4$  phase was formed, the materials were in one lattice, and it has cubic shape structures. Sintering process affects particle bulk size; a higher sintering temperature increases particle bulk size. Materials with holding time sintered that formed a single  $\text{Mn}_{0.8}\text{Zn}_{0.2}\text{Fe}_2\text{O}_4$  phase had higher magnetic retentivity compared to materials before sintering. This is evident by magnetic saturation ( $M_s$ ) and magnetic remanence ( $M_r$ ) values that are higher than for materials with-

out sintering. In 3 hours holding time sintering, the sample has a magnetic saturation ( $M_s$ ) of 54.05 emu/g and a magnetic remanence ( $M_r$ ) 14.38 emu/g, higher than other variants.

Дослідження манган-цинкового фериту  $Mn_{0,8}Zn_{0,2}Fe_2O_4$  стали популярними завдяки його гарним магнетним властивостям у якості магнетом'якого матеріялу. Вивчення магнетних властивостей  $Mn_{0,8}Zn_{0,2}Fe_2O_4$ , особливо до та після процесу спікання, необхідні для визначення характеристик його магнетного матеріялу. Тому дане дослідження було зосереджено на характеристиках манган-цинкового фериту  $Mn_{0,8}Zn_{0,2}Fe_2O_4$  з використанням методи співосадження з варіаціями часу спікання у 3, 4 та 5 годин при 1100°C. Основними матеріялами, використаними в цім дослідженні, були оксид мангану (MnO), оксид цинку (ZnO) і оксид заліза ( $Fe_2O_3$ ). Рентгенівська дифракція, сканувальна електронна мікроскопія разом з енергодисперсійною рентгенівською спектроскопією та тести на магнетометрі з вібруючим зразком були використані для характеристики фази, морфології та магнетних властивостей.  $Mn_{0,8}Zn_{0,2}Fe_2O_4$  із процесом спікання протягом 3, 4 і 5 годин мав як результат розмір кристалітів, змінений до 70,4194 нм, 52,91546 нм і 26,45 нм. За час витримки процесу спікання утворилася єдина фаза  $Mn_{0,8}Zn_{0,2}Fe_2O_4$ , матеріяли перебували в одній ґратниці та мали структури кубічної форми. Процес спікання впливає на об'єм частинок; більш висока температура спікання збільшує розмір частинок. Матеріяли з витриманим часом печені, які утворювали єдину фазу  $Mn_{0,8}Zn_{0,2}Fe_2O_4$ , мали більш високу залишкову намагнетованість у порівнянні з матеріялами перед спіканням. Це видно за значеннями магнетного насити ( $M_s$ ) і залишкової магнетної індукції ( $M_r$ ), які вище, ніж для матеріялів без спікання. За час витримування протягом 3 годин зразок має магнетний насит ( $M_s$ ) у 54,05 е.м.о./г і залишкову магнетну індукцію ( $M_r$ ) у 14,38 е.м.о./г, що вище, ніж в інших варіантах.

Исследования марганец-цинкового феррита  $Mn_{0,8}Zn_{0,2}Fe_2O_4$  стали популярными благодаря его хорошим магнитным свойствам в качестве магнитомягкого материала. Изучения магнитных свойств  $Mn_{0,8}Zn_{0,2}Fe_2O_4$ , особенно до и после процесса спекания, необходимы для определения характеристик его магнитного материала. Поэтому данное исследование было сосредоточено на характеристиках марганцево-цинкового феррита  $Mn_{0,8}Zn_{0,2}Fe_2O_4$  с использованием метода соосаждения с вариациями времени спекания 3, 4 и 5 часов при 1100°C. Основными материалами, использованными в этом исследовании, были оксид марганца (MnO), оксид цинка (ZnO) и оксид железа ( $Fe_2O_3$ ). Рентгеновская дифракция, сканирующая электронная микроскопия совместно с энергодисперсионной рентгеновской спектроскопией и тесты в магнитометре с вибрирующим образцом были использованы для характеристики фазы, морфологии и магнитных свойств.  $Mn_{0,8}Zn_{0,2}Fe_2O_4$  с процессом спекания в течение 3, 4 и 5 часов имел результатом размер кристаллитов, изменённый до 70,4194 нм, 52,91546 нм и 26,45 нм. За время выдержки процесса спекания образовалась единая фаза  $Mn_{0,8}Zn_{0,2}Fe_2O_4$ , материалы находились в одной решётке и имели структуры кубической формы. Процесс спекания влияет на объём частиц; более высокая температура

спекания увеличивает размер частиц. Материалы с выдержанным временем спечённые, которые образовывали единственную фазу  $Mn_{0.8}Zn_{0.2}Fe_2O_4$ , имели более высокую остаточную намагниченность по сравнению с материалами перед спеканием. Это видно по значениям магнитного насыщения ( $M_s$ ) и остаточной магнитной индукции ( $M_r$ ), которые выше, чем для материалов без спекания. За время выдерживания в течение 3 часов образец имеет магнитное насыщение ( $M_s$ ) 54,05 э.м.е./г и остаточную магнитную индукцию ( $M_r$ ) 14,38 э.м.е./г, что выше, чем у других вариантов.

**Key words:** magnetic properties, manganese–zinc ferrite, co-precipitation, holding time.

**Ключові слова:** магнетні властивості, манган-цинковий ферит, співосадження, час витримки.

**Ключевые слова:** магнитные свойства, марганец-цинковый феррит, соосаждение, время выдержки.

(Received 12 April 2019)

## 1. INTRODUCTION

The rapid development in nanotechnology gained a lot of attention from researchers and scientists. Generally, nanotechnology defined as science and engineering in the creation of material, functional structure, as well as devices on a scale of 1–100 nanometers [1, 2]. The positive impact of the rapid development in nanotechnology helps to provide conveniences to humankind. Research results in nanotechnology can be applied to the various field of life, *e.g.*, biotechnology, biomedicine, electronics, industries, and optics [3–9].

One type of magnetic nanoparticles that widely researched is manganese–zinc (Mn–Zn) ferrite nanoparticle. Mn–Zn ferrite has spinel crystal structures with  $MFe_2O_4$  formula where  $M$  is divalent cation of 3d transition elements such as  $Zn^{2+}$ ,  $Co^{2+}$ ,  $Fe^{2+}$ ,  $Ni^{2+}$ ,  $Cu^{2+}$  or  $Mn^{2+}$ .  $MFe_2O_4$  nanoparticle study is interesting due to not only its unique magnetic and electrical properties, but also its stability towards temperature and chemical substances [10]. Between spinel ferrites such as  $NiFe_2O_4$ ,  $CoFe_2O_4$ ,  $MnFe_2O_4$ ,  $ZnFe_2O_4$ , and other,  $MnFe_2O_4$  and  $ZnFe_2O_4$  have their advantages. The  $ZnFe_2O_4$  nanoparticle has advantages, *e.g.*, high sensitivity in temperature, and superparamagnetic properties at temperatures of 20–80°C in 5–10 nm sizes [11]. The advantages of manganese ferrites ( $MnFe_2O_4$ ) are having an inverse spinel structure and superparamagnetic properties in 9 nm crystal size at room temperature [12].

Manganese–zinc ferrite ( $MnZnFe_2O_4$ ) is a zinc-ferrite-based

nanoparticle with formula  $(M,Zn)Fe_2O_4$  with  $M = Mn$ . A combination between  $Fe_2O_4$  and  $MnFe_2O_4$  containing 0.8 mol  $Mn^{2+}$  and 0.2 mol  $Zn^{2+}$  compositions formed  $Mn_{0.8}Zn_{0.2}Fe_2O_4$ .  $Mn_{0.8}Zn_{0.2}Fe_2O_4$  has a mixed spinel structure. Mn–Zn-ferrite nanoparticle is a part of soft magnetic and low losses material with high permeability. Mn–Zn ferrite is known because of its low Curie temperature, low anisotropy crystalline magnetic constant value, and low remaining magnetisation [13, 14]. MnZn ferrite has spinel structures with Fe ion in tetrahedral position (position A) and octahedral position (position B), while Mn and Zn ions are on tetrahedral positions (position A) [15]. Based on the above advantages,  $Mn_{0.5}Zn_{0.5}Fe_2O_4$  has a high potential for high-frequency applications (inductor and transformer), data saving, and magnetic amplifier [16]. These were the base on choosing  $Mn_{0.5}Zn_{0.5}Fe_2O_4$  with the purpose of finding more optimised magnetic properties.

Mn–Zn ferrite nanoparticle can be synthesized by several means, *e.g.*, co-precipitation, thermal decomposition, hydrothermal, sol–gel, milling, *etc.* [9, 17, 18]. Each synthesis method has advantages and disadvantages. This research used the co-precipitation method, which is widely chosen because of its simplicity in the process and the lower cost usage compared to other methods. Co-precipitation method is also widely used to create magnetic nanoparticle to increase homogeneity, purity, and reactivity [19, 20].

In the co-precipitation method, synthesis parameters such as pH, temperature, and sintering-process holding time have crucial roles in controlling the particle size [17], [20].  $Mn_{0.4}Zn_{0.6}Fe_2O_4$  particle size increases along with the increase in sintering temperature that resulted in the rise of magnetisation. The correlation shows that magnetic properties depended on particle size [21].

Sintering with holding time variations also play a role in manganese–zinc ferrite with material. Therefore, the particle size is one of the important parameters to determine ferrite alloy magnetic properties.

## 2. RESEARCH METHOD

This research is experimental laboratory-type research carried out in the form of description. To obtain descriptive results on phase characterisation, morphology, and gauging manganese–zinc ferrite ( $MnZnFe_2O_4$ ) powder magnetic properties; this research used co-precipitation method with molar ratio  $Mn_{0.8}Zn_{0.2}Fe_2O_4$ . The component materials were manganese oxide (MnO), zinc oxide (ZnO), and iron oxide ( $Fe_2O_3$ ). All materials were mixed and added ethylene glycol as a solvent, then added 5 M concentration of sodium hydroxide at pH 12. The independent variables were the sintering

process with holding time of 3, 4, and 5 hours variations at temperature of  $1100^\circ\text{C}$ . Characterisation tests used XRD (X-Ray Diffraction) to determine formed phase, SEM-EDX (Scanning Electron Microscopy) to determine the material bulk size, and VSM (Vibrating Sample Magnetometer) to determine magnetic retentivity.

### 3. RESULTS AND DISCUSSION

In Figure 1, there is an increase in the highest peak between manganese-zinc ferrite ( $\text{Mn}_{0.8}\text{Zn}_{0.2}\text{Fe}_2\text{O}_4$ ) according to the XRD results. Unsintering process in manganese-zinc ferrite ( $\text{Mn}_{0.8}\text{Zn}_{0.2}\text{Fe}_2\text{O}_4$ ) material did not form single  $\text{MnZnFe}_2\text{O}_4$  phase and not in one lattice because crystal phase was not formed due to hematite ( $\text{Fe}_2\text{O}_3$ ) phase domination in the peaks. In 3, 4, and 5 hours holding time sintered at  $1100^\circ\text{C}$ , hematite ( $\text{Fe}_2\text{O}_3$ ) phase was declining, shown by the decreasing peaks and single  $\text{MnZnFe}_2\text{O}_4$  phase in the peak. In sintering 3, 4, and 5 hours holding-time variations at temperature of  $1100^\circ\text{C}$ , materials formed a single  $\text{MnZnFe}_2\text{O}_4$  phase that meant material was in one lattice with cubic shape crystal. Manganese-zinc ferrite material at  $1000^\circ\text{C}$  only showed  $\text{MnZnFe}_2\text{O}_4$  phase [18]. Unsintering process did not form single  $\text{MnZnFe}_2\text{O}_4$  phase nanoparticle, however, holding-time variations in 3, 4, and 5 hours formed single  $\text{MnZnFe}_2\text{O}_4$  phase nanoparticle as an effect of the sintering temperature that made hematite ( $\text{Fe}_2\text{O}_3$ ) phase decreased.

From Table 1 can be observed that unsintering manganese-zinc ferrite ( $\text{Mn}_{0.8}\text{Zn}_{0.2}\text{Fe}_2\text{O}_4$ ) crystal has 70.1496 nm in size that formed hematite ( $\text{Fe}_2\text{O}_3$ ) phase at the peaks, while sintered 3, 4, and 5

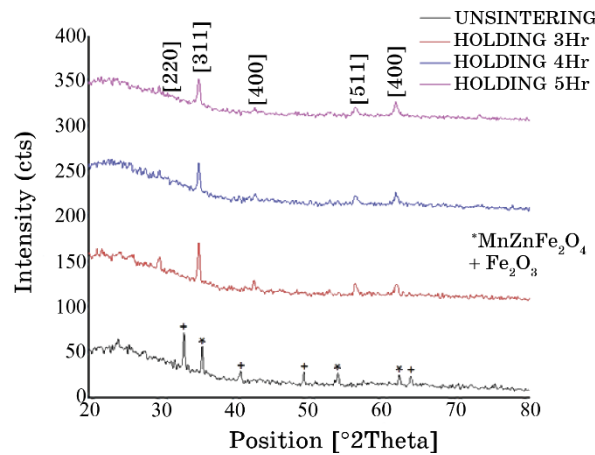


**Fig. 1.** XRD results of unsintered and sintered 3, 4, and 5 hours holding time.

hours holding-time variations have crystal size of 52.91546 nm, 26.45 nm, and 26.45014 nm, respectively, that formed single  $\text{MnZnFe}_2\text{O}_4$  phase at the peaks. In other words, the smallest particle size is found in sintered 4 hours holding time with crystal size of 26.45 nm. At temperature of  $1100^\circ\text{C}$ , crystallite size results became smaller until sintered 4 hours holding time.

Scanning electron microscopy (SEM) test aimed to analyse and compare the morphology and particle size of manganese–zinc ferrite

**TABLE 1.** Position value, FWHM, *D*-spacing, and crystallite size on manganese–zinc ferrite ( $\text{Mn}_{0.8}\text{Zn}_{0.2}\text{Fe}_2\text{O}_4$ ).

Variations	Pos. [ $^\circ 2\theta$ ]	Height [cts]	FWHM	Crystallite size, nm
unsintering	32.9617	45.55	0.1181	70.1496
3 jam	34.9596	47.26	0.1574	52.91546
4 jam	34.9689	31.02	0.3149	26.45
5 jam	34.9708	29.75	0.3149	26.45014

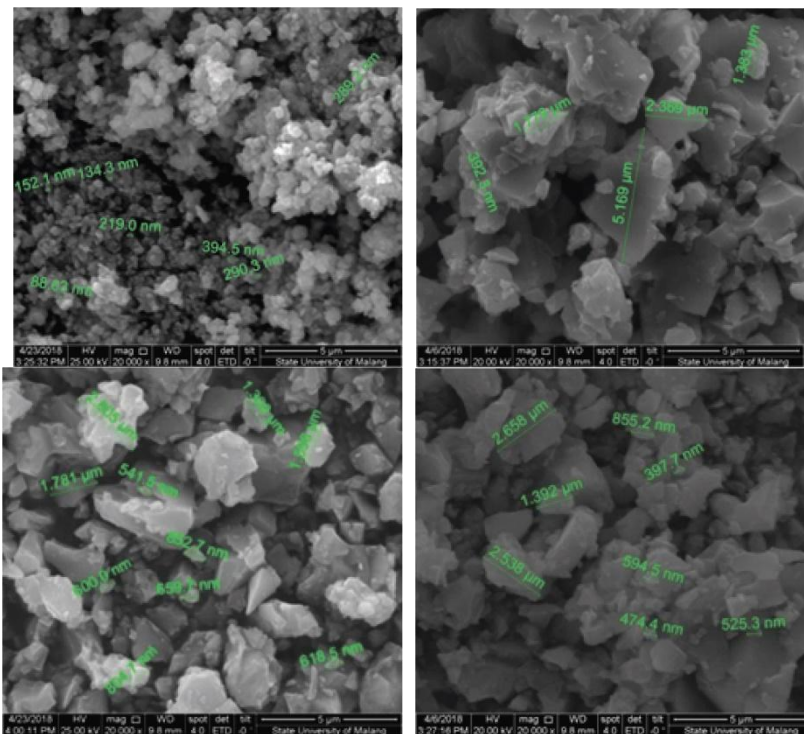


**Fig. 2.** Morphology of manganese–zinc ferrite ( $\text{Mn}_{0.8}\text{Zn}_{0.2}\text{Fe}_2\text{O}_4$ ) unsintered and 3, 4, and 5 hours holding time sintered in  $\times 20\,000$  magnifications.

( $\text{Mn}_{0.8}\text{Zn}_{0.2}\text{Fe}_2\text{O}_4$ ) material. In Figure 2, identification results from manganese–zinc ferrite ( $\text{Mn}_{0.8}\text{Zn}_{0.2}\text{Fe}_2\text{O}_4$ ) are that unsintering process has a particle size below 150 nm, while sintering process with 3, 4, and 5 hours holding time has an average particle size above 250 nm that homogenous with intergranular fracture and particle agglomeration. Result from 5 hours holding time sintered with standard deviation value 125.4187 nm shows that this variation has better homogeneity level than other sintered holding time variations. Sintering temperature affects the particle size of the material because sintering causes the particles to react and bind. A rise in sintering temperature is resulting in the increasing size of the particle in manganese–zinc ferrite material [22, 23], whereas stated in [16], the manganese–zinc ferrite material with annealing treatment at 400°C, 600°C and 1200°C shows bigger particle size along with higher sintering temperature.

VSM test for manganese–zinc ferrite ( $\text{Mn}_{0.8}\text{Zn}_{0.2}\text{Fe}_2\text{O}_4$ ) with sintering holding-time variations can be found in Fig. 3. During unsintering process, the magnetic saturation ( $M_s$ ) of 3.4 emu/g, magnetic remanence ( $M_r$ ) of 0.87 emu/g, and coercive-field strength ( $H_c$ ) of 0.0323 T were found. Magnetic properties in unsintered materials are quite low as evident by a low or almost flat curve. In 3 hours holding time sintered, magnetic saturation ( $M_s$ ) of 54.05 emu/g, magnetic remanence ( $M_r$ ) of 14.83 emu/g, and coercive field ( $H_c$ ) of 0.0199 T were found. This variation shows better magnetic properties than unsintered material, and the curve shows a rise in  $M_r$  value. In 4 hours holding time sintered, magnetic saturation ( $M_s$ ) of 51.7 emu/g, magnetic remanence ( $M_r$ ) of 12.95 emu/g, and coercive field ( $H_c$ ) of 0.0191 T were found. This variation shows a decline in magnetic properties compared to 3 hours variation as

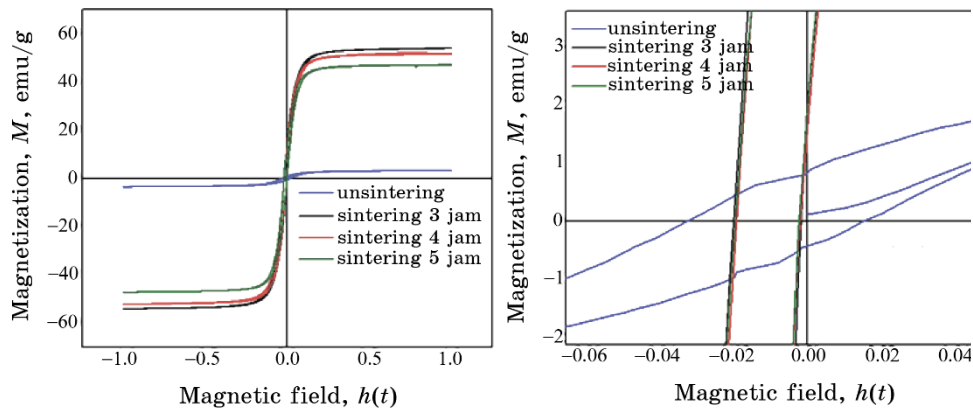


**Fig. 3.** VSM test results on manganese–zinc ferrite ( $\text{Mn}_{0.8}\text{Zn}_{0.2}\text{Fe}_2\text{O}_4$ ) unsintered and 3, 4, and 5 hours holding time sintered graphic.

**Table 2.** Values of  $M_s$ ,  $M_r$ , and  $H_c$  for the manganese–zinc ferrite ( $\text{Mn}_{0.8}\text{Zn}_{0.2}\text{Fe}_2\text{O}_4$ ) material.

Variations	$M_s$ , emu/g	$M_r$ , emu/g	$H_c$ , T	Crystallite size, nm
Unsintering	3.4	0.87	0.0323	70.1496
3 Jam	54.05	14.83	0.0199	52.91546
4 Jam	51.7	12.95	0.0191	26.45
5 Jam	47.11	12.7	0.0195	26.45014

evident in the  $M_r$  curve drop. In 5 hours holding time sintered, magnetic saturation ( $M_s$ ) of 47.11 emu/g, magnetic remanence ( $M_r$ ) of 12.7 emu/g, and coercive field ( $H_c$ ) of 0.0195 T were found. This variation shows a decline in magnetic properties compared to 4 hours variation as seen in the drop in  $M_r$  curve.

Table 2 shows that manganese–zinc ferrite ( $\text{Mn}_{0.8}\text{Zn}_{0.2}\text{Fe}_2\text{O}_4$ ) materials unsintered and sintered have superparamagnetic properties. Variation with 3 hours holding time had a more optimised magnetic properties than unsintered and 4 and 5 hours sintered variations. It has magnetic saturation ( $M_s$ ) of 54.05 emu/g and magnetic remanence ( $M_r$ ) of 14.83 emu/g with crystallite size of 52.91546 nm due to the higher  $M_s$  and  $M_r$ . It has cubic crystal structures. The crystal size becomes smaller along with the additional sintering duration. Duration also affects the  $M_s$  and  $M_r$  values because the smaller crystallite induces a lower electromagnetic field to alter the spin direction of an electron in the sample orbital magnetic moment, as long as there was a single  $\text{MnZnFe}_2\text{O}_4$  phase in the peak phase as an indication of the material crystallisation and one lattice. Magnetic saturation ( $M_s$ ) is also affected by the amount of Mn in  $\text{Mn}_{0.2}\text{Zn}_{0.8}\text{Fe}_2\text{O}_4$  and  $\text{Mn}_{0.8}\text{Zn}_{0.2}\text{Fe}_2\text{O}_4$  [22]. Magnetic saturation ( $M_s$ ) and magnetic remanence ( $M_r$ ) increased along with sintering temperature [24]. Materials at 1100°C and 2 hours holding time sintered showed the highest magnetic saturation ( $M_s$ ) of 73.64 emu/g and magnetic remanence ( $M_r$ ) of 2.20 emu/g compared to other sintering temperatures (800°C, 900°C, 1000°C). In conclusion, additional holding time in the sintering process results in the smaller crystallite size that made magnetic saturation ( $M_s$ ) and magnetic remanence ( $M_r$ ) dropped.

#### 4. CONCLUSION

Manganese–zinc ferrite ( $\text{Mn}_{0.8}\text{Zn}_{0.2}\text{Fe}_2\text{O}_4$ ) material using co-precipitation method with sintering holding-time variations has cubic crystal structures. Its hematite ( $\text{Fe}_2\text{O}_3$ ) phase drops as seen in the declination peaks and shows single  $\text{MnZnFe}_2\text{O}_4$  phase in the peak

phase. Sintering with 4 hours holding time, material has the smallest crystallite size of 26.45 nm compared to 52.915 nm from 3 hours holding time sintered and 26.45014 nm from 5 hours holding time sintered.

Morphology results of unsintering manganese–zinc ferrite ( $\text{Mn}_{0.8}\text{Zn}_{0.2}\text{Fe}_2\text{O}_4$ ) have a particle size below 150 nm, whereas the sintering with 3, 4, and 5 hours holding time gives an average size of above 350 nm and homogenous with intergranular fracture and particles' agglomeration. In 5 hours holding time sintered, it is standard deviation of 125.4187 nm indicating a better homogeneity level than other sintered variations. The increase in sintering temperature affects the material-particle size, and the increase in sintering temperature results in the greater manganese–zinc ferrite particle [22].

Manganese–zinc ferrite ( $\text{Mn}_{0.8}\text{Zn}_{0.2}\text{Fe}_2\text{O}_4$ ) with 3 hours holding time has an optimised magnetic properties compared to unsintered and 4 and 5 hours holding time sintered variations. Its magnetic saturation ( $M_s$ ) is of 54.05 emu/g, the magnetic remanence ( $M_r$ ) is of 14.83 emu/g, and the crystallite size is of 52.91546 nm. The resulting manganese–zinc ferrite ( $\text{Mn}_{0.8}\text{Zn}_{0.2}\text{Fe}_2\text{O}_4$ ) material has cubic crystal structures. Crystallite size becomes smaller along with longer sintering process that affects its magnetic saturation ( $M_s$ ) and magnetic remanence ( $M_r$ ). The smaller crystallite in sintering holding time variations requires the low electromagnetic field to alter the spin direction of an electron in the orbital magnetic moment. It is important to note that single  $\text{MnZnFe}_2\text{O}_4$  phase was formed as peak phase, indicating crystallised material and one lattice.

## REFERENCES

1. M. Abdullah, *Pengantar Nanosains* (Bandung: Penerbit ITB: 2009).
2. G. Schmid, *Nanotechnology: Principles and Fundamentals* (Weinheim: Wiley-VCH Verlag GmbH & Co. KGaA: 2008), vol. 1.
3. M. Gurumoorthy, K. Parasuraman, M. Anbarasu, and K. Balamurugan, *Nanoparticles by Chemical Co-Precipitation Method*, 5, No. 4: 63 (2015).
4. M. Tadic, S. Kralj, M. Jagodic, D. Hanzel, and D. Makovec, *Appl. Surf. Sci.*, 322: 255 (2014).
5. B. Ramaswamy et al., *Nanomedicine Nanotechnology, Biol. Med.*, 11, No. 7: 1821 (2015).
6. A. H. Lu, E. L. Salabas, and F. Schüth, *Angew. Chemie—Int. Ed.*, 46, No. 8: 1222 (2007).
7. L. He, M. S. Wang, J. P. Ge, and Y. D. Yin, *Acc. Chem. Res.*, 45, No. 9: 1431 (2012).
8. B. Gleich and J. Weizenecker, *Nature*, 435, No. 7046: 1214 (2005).
9. A. Dehghanhadikolaie, J. Ansary, and R. Ghoreishi, *Proc. Nat. Res. Soc.*, 2, No. 6: 02008 (2018).

10. M. Javad et al., *J. Magn. Magn. Mater.*, **321**: 152 (2009).
11. R. R. Shahraki, M. Ebrahimi, S. A. S. Ebrahimi, and S. M. Masoudpanah, *J. Magn. Magn. Mater.*, **324**, No. 22: 3762 (2012).
12. R. R. Muslim, *Magnetic Properties of Manganese Ferrite Nanoparticles: Thesis* (India: Thapar University: 2012).
13. I. Sharifi, H. Shokrollahi, and S. Amiri, *J. Magn. Magn. Mater.*, **324**, No. 6: 903 (2012).
14. H. Shokrollahi, *J. Magn. Magn. Mater.*, **320**, Nos. 3–4: 463 (2008).
15. A. Zapata and G. Herrera, *Ceram. Int.*, **1**: 2013.
16. P. Hu et al., *J. Magn. Magn. Mater.*, **322**, No. 1: 173 (2010).
17. R. Desai, V. Davariya, and K. Parekh, *Pramana*, **73**, No. 4: 765 (2009).
18. W. H. Lee, C. S. Hong, and S. Y. Chang, *Archives of Metallurgy and Materials*, **60**: Iss. 2: 9 (2015).
19. C. Venkataraju and R. Paulsingh, *Journal of Nanoscience*, **2014**: 5 (2014).
20. P. Puspitasari, A. Muhammad, H. Suryanto, and A. Andoko, *High Temp. Mater. Process. An Int. Q. High-Technology Plasma Process.* (2018), vol. **22**, p. 239.
21. P. Mathur, A. Thakur, and M. Singh, *J. Magn. Magn. Mater.*, **320**, No. 7: 1364 (2008).
22. P. Puspitasari et al., *Materials Science Forum*, **857**: 146 (2016).
23. N. Yahya and P. Puspitasari, *J. Nano Res.*, **21**: 131 (2012).
24. M. M. Rashad and M. I. Nasr, *Nanopowders Synthesized by Co-Precipitation Method*, **8**, No. 3: 325 (2012).